

Bending Strength of Piezoelectric Ceramics and Single Crystals for Multifunctional Load-Bearing Applications

Steven R. Anton, Alper Erturk, and Daniel J. Inman

Abstract—The topic of multifunctional material systems using active or smart materials has recently gained attention in the research community. Multifunctional piezoelectric systems present the ability to combine multiple functions into a single active piezoelectric element, namely, combining sensing, actuation, or energy conversion ability with load-bearing capacity. Quantification of the bending strength of various piezoelectric materials is, therefore, critical in the development of load-bearing piezoelectric systems. Three-point bend tests are carried out on a variety of piezoelectric ceramics including soft monolithic piezoceramics (PZT-5A and PZT-5H), hard monolithic ceramics (PZT-4 and PZT-8), single-crystal piezoelectrics (PMN-PT and PMN-PZT), and commercially packaged composite devices (which contain active PZT-5A layers). A common 3-point bend test procedure is used throughout the experimental tests. The bending strengths of these materials are found using Euler-Bernoulli beam theory to be 44.9 MPa for PMN-PZT, 60.6 MPa for PMN-PT, 114.8 MPa for PZT-5H, 123.2 MPa for PZT-4, 127.5 MPa for PZT-8, 140.4 MPa for PZT-5A, and 186.6 MPa for the commercial composite. The high strength of the commercial configuration is a result of the composite structure that allows for shear stresses on the surfaces of the piezoelectric layers, whereas the low strength of the single-crystal materials is due to their unique crystal structure, which allows for rapid propagation of cracks initiating at flaw sites. The experimental bending strength results reported, which are linear estimates without nonlinear ferroelastic considerations, are intended for use in the design of multifunctional piezoelectric systems in which the active device is subjected to bending loads.

I. INTRODUCTION

PIEZOELECTRIC materials used as sensors, actuators, and energy conversion devices have been reported extensively in the literature [1], [2]. One of the more significant challenges in designing systems using piezoelectric ceramics and single crystals is their brittle nature, leading to susceptibility to failure under the application of mechanical or electrical loads. Recently, the topic of multifunctionality in material and energy systems has gained significant

interest in the research community [3]. In such systems, it is common for an active material to support mechanical loading in a structure to provide multifunctionality. In the design of multifunctional piezoelectric systems in which the active elements are subjected to large mechanical loading, it becomes necessary to accurately quantify the strength of the piezoelectric devices to ensure proper operation without failure.

Multifunctional load-bearing piezoelectric systems can be found in vibration energy harvesting applications where the active piezoelectric material is used not only to harvest ambient vibration energy, but also to support structural loading in the system. An early example of such a system can be found in the work by Shenck and Paradiso, in which piezoelectric material is inserted into a shoe to harvest energy from human walking [4]. The piezoelectric devices are used to generate electrical energy, but also serve as part of the sole of the shoe, thus supporting the load imposed by the user. More recently, researchers have investigated multifunctional piezoelectric harvesting in unmanned aerial vehicle applications in which piezoelectric elements are proposed as landing gear [5]. Other examples in which piezoelectric ceramics are subjected to bending loads include passive [6] and active [7] damping treatment of lightweight structures, such as aircraft components excited by aerodynamic loading. Finally, the authors have developed the concept of self-charging structures, in which a single composite structure composed of piezoelectric elements, thin-film battery elements, and a substrate can be used to simultaneously harvest vibration energy, store the harvested energy, and support mechanical load [8]. In each of these examples, large mechanical loading is imposed upon the active piezoelectric elements, thus the strength of the piezoelectric materials is critical in the design of the system.

Previous research exists in both the ceramics and smart structures fields in which the bending strength of piezoelectric materials has been investigated. Studies have analyzed the bending strength of soft monolithic piezoceramic [PIC 151 lead zirconate titanate (PZT) from PI Ceramic GmbH, Lederhose, Germany] under various poling states with results showing a decrease in strength for poled samples [9], [10]. The effects of varying electric field on the same material have also been investigated for various poling states and results suggest that polarization parallel to the length of the specimen greatly reduces strengths, polarization through the thickness of the specimen decreases strength slightly, and the application of an electric field

Manuscript received November 13, 2011; accepted March 3, 2012. The authors gratefully acknowledge the support of the Air Force Office of Scientific Research MURI under Grant No. F9550-06-1-0326 "Energy Harvesting and Storage Systems for Future Air Force Vehicles," monitored by Dr. B. L. Lee.

S. R. Anton is with the Engineering Institute, Los Alamos National Laboratory, Los Alamos, NM (e-mail: sranton@lanl.gov).

A. Erturk is with the George W. Woodruff School of Mechanical Engineering, Georgia Institute of Technology, Atlanta, GA.

D. J. Inman is with the Department of Aerospace Engineering, The University of Michigan, Ann Arbor, MI.

DOI <http://dx.doi.org/10.1109/TUFFC.2012.2299>

significantly reduces strength in both tension and bending [11], [12]. Research has also been performed to study the effects of varying temperature as well as electric field on the bending strength of hard PZT ceramics (APC-841 PZT, APC International Inc., Mackeyville, PA) [13]. Bend testing results show that the bending strength decreases significantly with increasing temperature and also exhibits large decreases under applied electric fields, in agreement with [11] and [12]. Three-point bend testing of unpoled lead magnesium niobate–lead titanate (PMN-29%PT) single-crystal ceramic manufactured by H.C. Materials Corp. (Urbana, IL) has been reported in the literature, however, samples were not loaded to failure, thus bending strength results were not presented [14]. The bending strength of lead indium niobate–lead magnesium niobate–lead titanate (PIN-PMN-PT) single crystals has also been investigated with respect to applied electric field as well as surface condition [15]. Results show a decrease in strength with the application of electric field, an increase in strength with surface polishing, and a significant increase in strength with surface and edge polishing. Lastly, it has been shown in the literature that nonlinear deformations occur in the bending of ferroelectric materials [16]. Nonlinear models based on the work of Nadai [17] have been presented to describe this phenomenon in piezoelectric materials [12].

The goal of this research is to present a comprehensive, yet basic, study of the bending strength of several commonly used poled piezoelectric materials that can be utilized in the design of multifunctional load-bearing applications. Linear formulations for bending strength based on Euler-Bernoulli beam theory are utilized in this work to provide a general analysis of the bending strength of a wide variety of piezoelectric materials, where details of the nonlinear response of the materials are not investigated. Eight piezoceramic materials/devices are investigated in this work: two soft PZT materials, two hard PZT materials, two single-crystal piezoelectric materials, and two commercially packaged piezoceramic devices. The results presented in this paper can be used as an engineering design tool in the development of multifunctional piezoelectric applications.

II. EXPERIMENTAL PROCEDURES

A. Materials

Several commonly used piezoelectric materials are investigated in this work. Two types of soft PZT ceramic materials, PZT-5A (DOD Type II) and PZT-5H (DOD Type VI) ceramics (PSI-5A4E and PSI-5H4E, respectively) manufactured by Piezo Systems Inc. (Cambridge, MA), are investigated. The PZT-5A material is characterized by the manufacturer as having piezoelectric constants $d_{33} = 390$ pC/N and $d_{31} = -190$ pC/N, density $\rho = 7800$ kg/m³, and Curie temperature 350°C. The PZT-5H material has piezoelectric constants $d_{33} = 650$ pC/N and $d_{31} =$

-320 pC/N, density $\rho = 7800$ kg/m³, and Curie temperature 230°C. Both materials use vacuum-sputtered nickel electrodes and are poled through the thickness. Several researchers have used these PZT ceramics in energy-harvesting applications, including PZT-5A for self-powered sensor nodes [18] and gunfire shock munitions harvesting [19], and PZT-5H for microgenerators in wireless electronics [20].

Two types of hard PZT ceramics are also tested. PZT-4 (DOD Type I) and PZT-8 (DOD Type III) ceramics (PZT-844 and PZT-881, respectively) manufactured by APC International Inc. are studied. The materials utilize silver electrodes and are poled through the thickness. PZT-844 has a reported piezoelectric constant $d_{33} = 300$ pC/N, density $\rho = 7700$ kg/m³, and Curie temperature 320°C, and PZT-881 has piezoelectric constant $d_{33} = 260$ pC/N, density $\rho = 7600$ kg/m³, and Curie temperature 310°C. Although hard PZT is typically used in high-power ultrasonic and sonar applications, PZT-4 has recently been proposed for use in harvesting magnetic energy through the combination of piezoelectric and piezomagnetic material layers in a composite device [21].

In addition to conventional PZT ceramics, two types of single-crystal piezoelectric materials are also investigated in this research. PMN-PT (PMN-29PT) single crystals and PMN-PZT single crystals (CPSC 160–95) produced by Ceracomp Co. Ltd. (Cheonan, Korea) are tested. The materials contain gold electrodes and are poled through the thickness. According to the manufacturer, the PMN-PT single crystals have piezoelectric constants $d_{33} = 1500$ pC/N and $d_{32} = 1350$ pC/N, rhombohedral–tetrahedral (R–T) transition temperature 90°C, and Curie temperature 130°C. The PMN-PZT samples have reported piezoelectric constants $d_{33} = 2000$ pC/N and $d_{32} = 1850$ pC/N, R–T transition temperature 95°C, and Curie temperature 160°C. Details on the fabrication and experimental testing of the electrical properties of the Ceracomp PMN-PZT single crystals are given by Lee *et al.* [22] and Zhang *et al.* [23]. Several researchers have investigated the use of PMN-PT in energy harvesting applications to utilize its large piezoelectric coupling [24], [25]. Although a relatively new material, some research has been conducted to investigate the use of PMN-PZT single-crystal materials for energy harvesting applications [26], [27].

The final types of piezoelectric material investigated in this paper are commercially packaged composite devices. QuickPack piezoelectric devices (QP10n and QP16n) manufactured by Midé Technology Corp. (Medford, MA) are examined; they contain PZT-5A (3195HD manufactured by CTS Corp., Albuquerque, NM) active elements bracketed by 0.0635-mm-thick Kapton layers (bonded with high-shear-strength epoxy) with embedded copper-foil electrodes. The PZT-5A material, poled through the thickness, has piezoelectric constants $d_{33} = 390$ pC/N and $d_{31} = -190$ pC/N, density $\rho = 7800$ kg/m³, and Curie temperature 350°C. The packaged QuickPack devices offer the benefit of added mechanical support through the use of the Kapton layers, and convenient electrode configura-

TABLE I. PHYSICAL DIMENSIONS OF VARIOUS PIEZOELECTRIC MATERIALS TESTED.

Material	Manufacturer part number	Bulk dimensions (mm)	Final sample dimensions (mm)
PZT-5A	T110-A4E-602	72.4 × 72.4 × 0.267	36.18 × 1.959 × 0.267
PZT-5H	T110-H4E-602	72.4 × 72.4 × 0.267	36.18 × 1.959 × 0.267
PZT-4	PZT-844	40.0 × 10.0 × 0.5	20.0 × 1.950 × 0.5
PZT-8	PZT-881	25.4 × 25.4 × 1.0	25.4 × 1.914 × 1.0
PMN-PT	PMN-29PT	30.0 × 2.012 × 0.28	30.0 × 2.012 × 0.28
PMN-PZT	CPSC 160-95	40.0 × 10.0 × 0.28	40.0 × 1.967 × 0.28
QuickPack	QP10n	46.0 × 20.6 × 0.254	46.0 × 1.962 × 0.254
QuickPack	QP16n	46.0 × 20.6 × 0.152	46.0 × 1.960 × 0.152

ration from the manufacturer. Previous research studies have investigated the energy harvesting ability of Quick-Pack devices [28], and QuickPacks have been used in the self-charging structures proposed by the authors [29]–[31].

B. Sample Preparation

All of the materials used in this study are supplied as bulk material from the manufacturers, with the exception of the PMN-PT samples, which are supplied as beam-like specimens that do not require further processing. The physical dimensions and the manufacturer part numbers for all of the materials tested in this work are given in Table I. Typical bend test specimens are beam-like, with large aspect ratios; thus, processing of the bulk material is required to obtain appropriate samples for testing. The ASTM C 1161-02c standard was consulted in preparing the test samples [32]. Samples with dimensions of $4 \times 3 \times 45$ mm are specified in the standard, however, the thicknesses of the materials acquired in this study dictate a deviation from the standard. To maintain beam-like samples, the bulk material is cut using a diamond-blade dicing saw to provide samples of approximately 2 mm width. A MicroAutomation Inc. 1006 dicing saw (Sunnyvale, CA) is used with 2- to 6- μ m grit, 75- μ m-wide diamond dicing blades, a spindle speed of 28000 rpm, and a feed rate of 2 mm/s. The length of the samples varies from 20.0 to 46.0 mm across the different material types. After completion of the dicing operation, the samples are investigated using a Nikon Instruments Inc. (Melville, NY) Eclipse LV100 optical microscope to obtain a precise measurement of the width of each sample, and additionally to

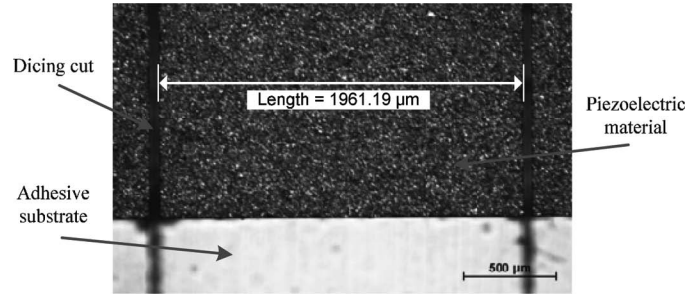


Fig. 1. Optical microscope image of the PMN-PZT sample after dicing showing the width measurement (5 \times objective lens).

determine the average flaw size induced in the edges from the dicing process. Fig. 1 shows an example of an image acquired using the optical microscope in which the width of a PMN-PZT sample has been measured. The final sample dimensions for each material are also listed in Table I. Characteristic images of the flaws induced during dicing are shown in Fig. 2, and the average flaw size is found to be about 6, 8, 40, 35, 19, and 19 μ m for PZT-5A, PZT-5H, PZT-4, PZT-8, PMN-PT, and PMN-PZT, respectively. The outer Kapton layers of the QuickPack devices prohibited optical measurement of flaw size in the piezoelectric layers. Fig. 3 shows the final prepared samples ready for bend testing.

C. Experimental Setup

Three-point bend testing is carried out using a 5848 MicroTester frame (Instron, Norwood, MA) equipped

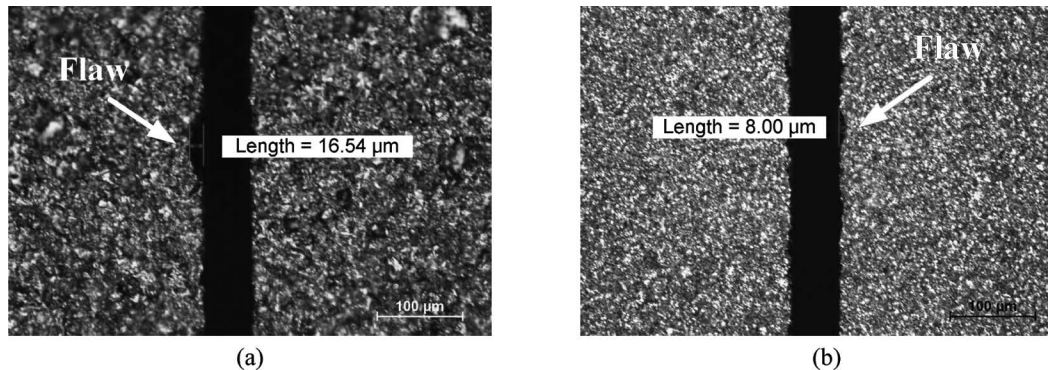


Fig. 2. Optical microscope images of (a) PMN-PZT and (b) PZT-5H samples showing flaw sizes (20 \times objective lens).

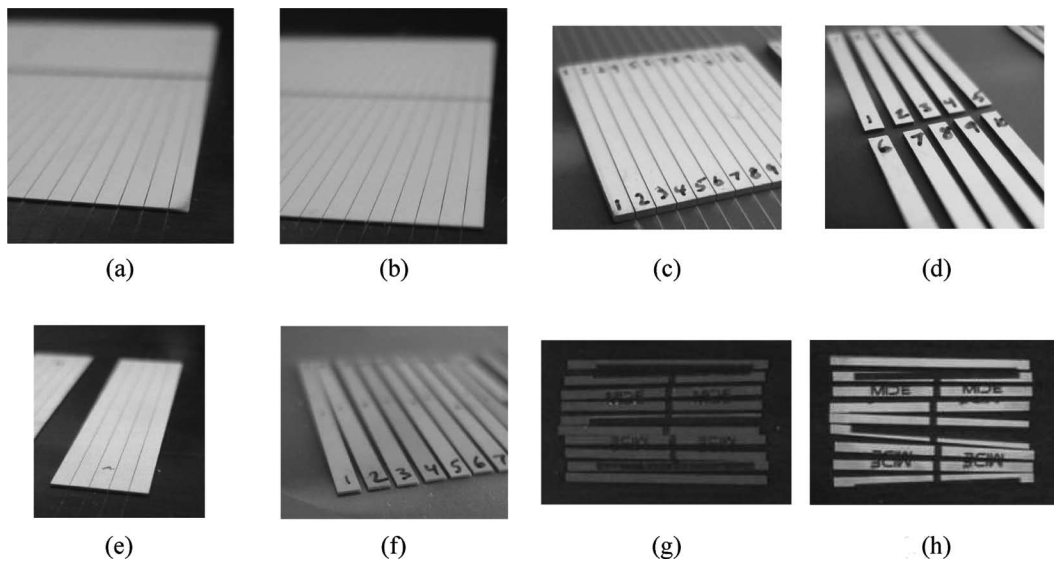


Fig. 3. Diced piezoelectric samples prepared for bending tests, including (a) PZT-5H, (b) PZT-5A, (c) PZT-8, (d) PZT-4, (e) PMN-PZT, (f) PMN-PT, (g) QP10n, and (h) QP16n.

with a 50-N load cell, along with a small 3-point bend fixture with adjustable lower supports, shown in Fig. 4. Per the ASTM C 1161–02c test standard, the crosshead rate for each test is specified to provide a strain rate of $1 \times 10^{-4} \text{ s}^{-1}$ using the following relation [32]:

$$\dot{\epsilon} = \frac{6hs}{L^2}, \quad (1)$$

where $\dot{\epsilon}$ is the strain rate, h is the thickness of the sample, s is the crosshead rate, and L is the support span. The number of samples, crosshead rate and support span for each type of material are listed in Table II. During each test, the load and crosshead displacement are recorded at a sampling rate of 50 Hz.

III. RESULTS AND DISCUSSION

Typical stress-strain curves recorded during the bending tests for each material investigated are shown in Fig. 5. It should be noted that the QP16n samples did not exhibit any internal cracking or failure throughout the entire displacement range of the test. Although both QuickPack devices contain identical types of PZT-5A inner layers, the piezoceramic layer contained in the QP16n samples is considerably thinner than that of the QP10n devices, thus the maximum curvature obtained during testing is not large enough to induce the strains needed for failure of the piezoceramic member in the QP16n samples. No failure data are obtained for the QP16n samples and the material will not be discussed further. The failure loads

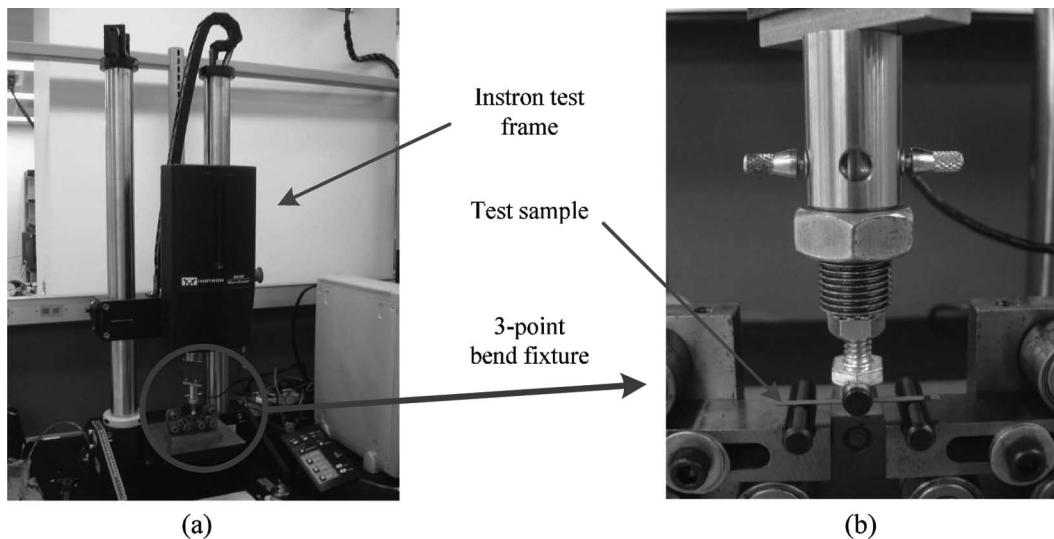


Fig. 4. Three-point bend test setup: (a) Instron 5848 MicroTester, (b) 3-point bend fixture.

TABLE II. VARIOUS TEST PARAMETERS FOR THE PIEZOELECTRIC MATERIALS INVESTIGATED.

Material	Number of samples	Crosshead rate (mm/min)	Support span (mm)
PZT-5A	50	2.341	25
PZT-5H	50	2.341	25
PZT-4	30	0.450	15
PZT-8	30	0.400	20
PMN-PT	30	2.232	25
PMN-PZT	10	3.214	30
QP10n	30	4.823	35
QP16n	30	8.059	35

observed during testing are used to determine the bending strength of each sample based on Euler-Bernoulli beam theory. For the homogeneous samples tested, the following formulation is used:

$$\sigma_b = \frac{3L}{2bh^2} P_f, \quad (2)$$

where P_f is the failure load, L is the support span, b is the sample width, and h is the sample thickness. For the QP10n composite material, the following relation is used to calculate the bending strength of the inner piezoelectric layer at failure:

$$\sigma_b = \frac{P_f L h_p E_p}{8EI}, \quad (3)$$

where h_p is the thickness of the central piezoelectric element, E_p is the elastic modulus of the piezoelectric material (PZT-5A), and EI is the bending stiffness of the composite structure. In each case, the failure load, P_f , is taken as the maximum load observed in the test for the materials exhibiting classic brittle failure (PZT-5A, PZT-5H, PZT-4, PZT-8, PMN-PT, and PMN-PZT), and as the first peak in the load, which occurs immediately before the initial cracking, in the QP10n material. Bending strengths calculated using the failure loads obtained from the experiments are presented in Fig. 6 for all materials tested. The following sections present a summary of the experimental results for each material investigated.

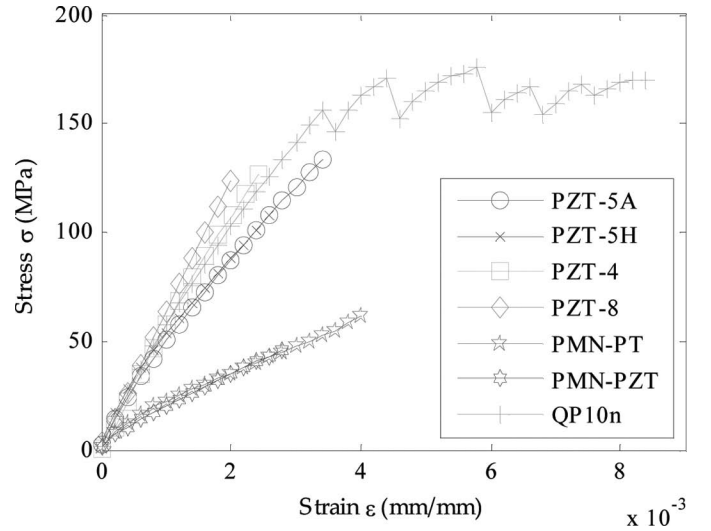


Fig. 5. Representative stress-strain curves from 3-point bending tests.

A. PZT-5A and PZT-5H Soft Ceramics

Both PZT-5A and PZT-5H materials exhibit similar brittle behavior during 3-point bend tests, which can be observed from the results shown in Fig. 5. Both materials follow a similar stress-strain trend with an abrupt failure that is characteristic to brittle materials, however, PZT-5H fails at a lower stress than PZT-5A. From the bending strength results shown in Fig. 6, it can be seen that the PZT-5H samples, on average, give lower strength values than PZT-5A over the entire sample set. Strength testing of ceramic materials often exhibits significant variability between samples [33]. The variabilities observed in the PZT-5A and PZT-5H strength data are quite reasonable, and the results are considered to be favorable.

B. PZT-4 and PZT-8 Hard Ceramics

From Fig. 5 it can be seen that both PZT-4 and PZT-8 samples exhibit brittle failure, as expected. Both materials fail at similar stress values that are between the failure stresses of the soft piezoceramics (PZT-5A and PZT-5H),

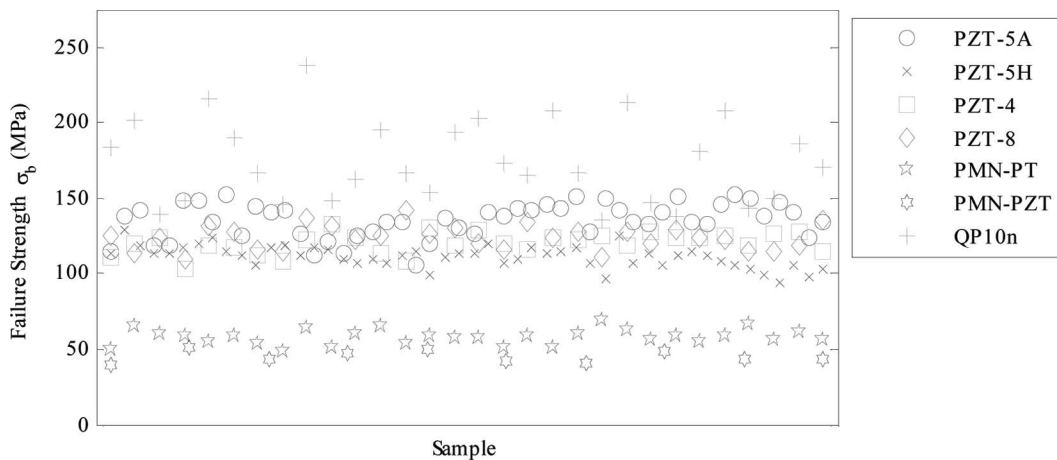


Fig. 6. Bending strength values calculated for various piezoceramic materials tested.

which is confirmed by the failure strength values presented in Fig. 6. Additionally, a fairly low amount of variation is observed in the failure data.

C. PMN-PT and PMN-PZT Single Crystals

As with the other monolithic ceramics tested, both PMN-PT and PMN-PZT samples fail in a brittle fashion, as shown in Fig. 5. The failure stress levels, however, are significantly lower than those of the other materials tested. The difference in strength can be explained by the unique crystal structure of the PMN-PT and PMN-PZT samples which allows for rapid propagation of cracks originating at flaw sites. The single-crystal samples are expected to yield lower bending strengths compared with the other ceramics investigated. The appeal of single-crystal piezoelectric materials lies in their large piezoelectric coupling coefficients compared with conventional piezoceramic materials. Variability in the bending strength results for PMN-PZT is also rather low and compares well to the results observed for the monolithic samples. Additionally, the bending strength of PMN-PT samples is higher than the bending strength of PMN-PZT samples.

D. QuickPack QP10n Composite

Stress-strain data for the QP10n samples exhibits some interesting behavior. Fig. 5 shows a typical curve obtained during bend testing in which the stress is observed to drop sharply after initial failure, however, recover and continue to exhibit several brittle failures while maintaining a fairly constant average stress. This unique behavior occurs for these samples because of the Kapton outer layers surrounding the inner PZT-5A layer. The brittle failures observed during the test are a result of the inner piezoceramic layer cracking, however, unlike the traditional monolithic and single crystal samples, the QP10n sample does not completely fail upon cracking of the PZT-5A layer. The outer Kapton film is able to maintain the integrity of the sample after cracking, and in fact, the composite structures never exhibit complete fracture because the Kapton is able to resist failure throughout the entire displacement range of the test. The maximum load observed immediately before the initial cracking is taken as the failure load for the QuickPack samples. Based on the failure strength data presented in Fig. 6, it can be observed that the average bending strength for the QuickPack samples is notably higher than those of the conventional ceramic materials. This can be attributed to the composite structure of the QuickPack devices, which includes high-shear-strength epoxy on the piezoceramic surfaces, resulting in surface shear stresses resisting the applied bending load. Additionally, the variability is significantly higher compared with those of the other materials. The increased variability is likely due to the non-uniformity of the test samples. The additional copper electrode layers of the QuickPack devices do not cover the entire surface of the device, hence some samples contained outer electrode layers whereas

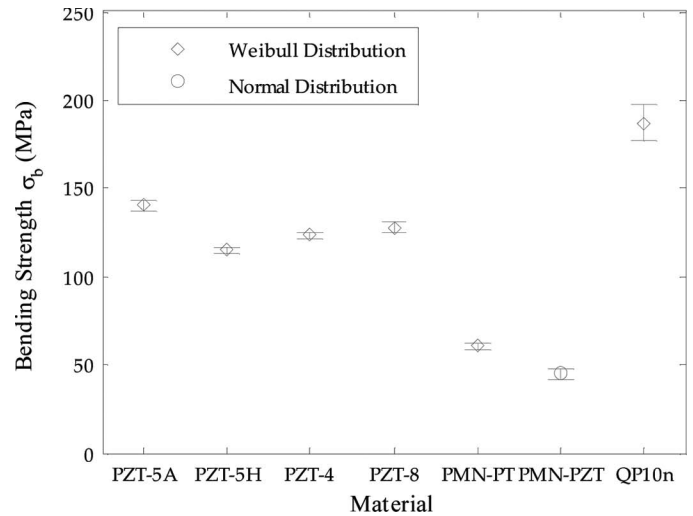


Fig. 7. Bending strength comparison for all samples tested.

others lacked such layers. Additionally, there may be non-uniform distribution of epoxy in the composite structures.

E. Statistical Analysis of Bending Strength Results

As a means of quantifying the average bending strength and variability of each material investigated, the bending strength data for each material is fit to a Weibull distribution, which is common practice for tensile and bending failure strengths of ceramic materials [33]. The Weibull distribution is described by the following cumulative distribution function:

$$F = 1 - \exp\left[-\left(\frac{\sigma_b}{\sigma_\theta}\right)^m\right], \quad (4)$$

where F is the probability of failure, σ_b is the failure strength, σ_θ is the Weibull characteristic strength, and m is the Weibull modulus. The Weibull distribution is left-skewed which better represents the flaw-dependent failure mode of ceramic materials as opposed to the standard normal distribution. The Weibull characteristic strength, σ_θ , provides an estimate of the strength observed over the entire sample set, and the Weibull modulus, m , gives a measure of the variability in the strength data, with a larger value of m corresponding to a smaller amount of variation in the data. As suggested in the ASTM C 1161–02c test standard, materials with sample sizes of 30 or more (PZT-5A, PZT-5H, PZT-4, PZT-8, PMN-PT, and QP10n) are fit to the Weibull distribution, where materials with sample sizes less than 30 (PMN-PZT) are fit to the normal distribution with simple mean and standard deviation calculations made [32]. Results of the statistical analysis for all materials tested are given in Fig. 7 and Table III, where both the Weibull characteristic strength and Weibull modulus (mean strength and standard deviation for PMN-PZT samples) are given with a 95% confidence interval on all terms. The results confirm the strength and variability trends described in the previous sections

TABLE III. BENDING STRENGTH PARAMETERS FOR ALL MATERIALS TESTED
WITH 95% CONFIDENCE INTERVAL IN BRACKETS.

Material	Weibull characteristic strength, σ_θ (MPa)	Weibull modulus, m
PZT-5A	140.4 [137.6;143.2]	14.6 [11.7;18.2]
PZT-5H	114.8 [112.8;116.9]	16.6 [13.5;20.3]
PZT-4	123.2 [121.0;125.5]	20.6 [15.6;27.1]
PZT-8	127.5 [124.6;130.5]	16.3 [12.6;21.1]
PMN-PT	60.6 [58.7;62.5]	12.1 [9.3;15.6]
QP10n	186.6 [176.5;197.3]	6.8 [5.2;8.9]
	Mean strength (MPa)	Standard deviation
PMN-PZT	44.9 [42.1;47.7]	3.9 [2.7;7.1]

and provide numerical measures of those properties. The Weibull characteristic strength of PZT-5A is slightly higher than the strength of PZT-5H, with values of 140.4 and 114.8 MPa, respectively. PZT-4 and PZT-8 have nearly identical strengths at 123.2 and 127.5 MPa, respectively, which lie between PZT-5A and PZT-5H. The strengths of the PMN-PT and PMN-PZT single-crystal samples are considerably lower than the other materials tested, with values of 60.6 and 44.9 MPa, respectively. The QuickPack QP10n samples exhibit the highest strength, with a value of 186.6 MPa.

IV. SUMMARY AND CONCLUSIONS

The bending strength of various common piezoelectric ceramics and single crystals was investigated to provide a basis for the design of multifunctional load-bearing piezoelectric systems. Eight piezoelectric materials were studied: PZT-5A and PZT-5H soft monolithic piezoceramics, PZT-4 and PZT-8 hard monolithic ceramics, PMN-PT and PMN-PZT single-crystal piezoelectrics, and Quick-Pack QP10n and QP16n commercially available packaged piezoceramic composite devices. A common 3-point bend test procedure was used to evaluate each material for comparison purposes. Bending strength results obtained from the testing showed a relatively small amount of variability for the monolithic and single-crystal piezoceramic samples tested. The strength of the PZT-5A samples (140.4 MPa) was slightly greater than that of the PZT-5H samples (114.8 MPa). The hard piezoceramics were found to have bending strengths between those of PZT-5A and PZT-5H, with the PZT-4 samples at 123.3 MPa and the PZT-8 samples at 127.5 MPa. The strength of the single-crystal samples is significantly less than the other monolithic materials, with PMN-PT at 60.6 MPa and PMN-PZT at 44.9 MPa. The bending strength values of the QP10n composite samples exhibited a considerable amount of variation and are much greater (186.6 MPa) than those of the monolithic materials, which is attributed to the high-shear-strength epoxy used to bond the PZT-5A and Kapton layers. Overall, the results of this research provide a foundation for the design of multifunctional piezoelectric systems in which the active device is used to support structural loading in the system.

ACKNOWLEDGMENTS

The authors acknowledge the support of C. Folgar from the Department of Materials Science and Engineering and Dr. D. Leber from the Department of Electrical and Computer Engineering at Virginia Tech.

REFERENCES

- [1] W. Keywang, K. Lubitz, and W. Wersing, *Piezoelectricity: Evolution and Future of a Technology*. New York, NY: Springer, 2008.
- [2] K. Uchino, "Piezoelectric actuators 2006," *J. Electroceram.*, vol. 20, no. 3-4, pp. 301-311, 2008.
- [3] L. Christodoulou and J. D. Venable, "Multifunctional material systems: The first generation," *JOM*, vol. 55, no. 12, pp. 39-45, 2003.
- [4] N. S. Shenck and J. A. Paradiso, "Energy scavenging with shoe-mounted piezoelectrics," *IEEE Micro*, vol. 21, no. 3, pp. 30-42, 2001.
- [5] A. Erturk, J. M. Renno, and D. J. Inman, "Modeling of piezoelectric energy harvesting from an L-shaped beam-mass structure with an application to UAVs," *J. Intell. Mater. Syst. Struct.*, vol. 20, no. 5, pp. 529-544, 2009.
- [6] S.-Y. Wu, T. L. Turner, and S. A. Rizzi, "Piezoelectric shunt vibration damping of an F-15 panel under high-acoustic excitation," in *Smart Structures and Materials 2000: Damping and Isolation*, 2000, pp. 276-287.
- [7] J. S. Browning, R. G. Cobb, R. A. Canfield, and S. K. Miller, "F-16 ventral fin buffet alleviation using piezoelectric actuators," in *50th AIAA/ASME/ASCE/AHS/ASC Structures, Structural Dynamics, and Materials Conf.*, 2009, art. no. AIAA 2009-2538.
- [8] S. R. Anton, A. Erturk, and D. J. Inman, "Multifunctional self-charging structures using piezoceramics and thin-film batteries," *Smart Mater. Struct.*, vol. 19, no. 11, art. no. 115021, 2010.
- [9] T. Fett, D. Munz, and G. Thun, "Tensile and bending strength of piezoelectric ceramics," *J. Mater. Sci. Lett.*, vol. 18, no. 23, pp. 1899-1902, 1999.
- [10] D. Munz, T. Fett, S. Muller, and G. Thun, "Deformation and strength behaviour of a soft PZT ceramic," *Proc. SPIE*, vol. 3323, pp. 84-95, 1998.
- [11] T. Fett, M. Kamlah, D. Munz, and G. Thun, "Strength of a PZT ceramic under different test conditions," *Proc. SPIE*, vol. 3992, pp. 197-208, 2000.
- [12] T. Fett, D. Munz, and G. Thun, "Bending strength of a PZT ceramic under electric fields," *J. Eur. Ceram. Soc.*, vol. 23, no. 2, pp. 195-202, 2003.
- [13] R. Fu and T.-Y. Zhang, "Influences of temperature and electric field on the bending strength of lead zirconate titanate ceramics," *Acta Mater.*, vol. 48, no. 8, pp. 1729-1740, 2000.
- [14] N. Di and D. J. Quesnel, "Photoelastic effects in Pb (Mg_{1/3}Nb_{2/3})O₃-29%PbTiO₃ single crystals investigated by three-point bending technique," *J. Appl. Phys.*, vol. 101, no. 4, art. no. 043522, 2007.
- [15] P. Zhao, S. Goljahi, W. Dong, T. Wu, P. Finkel, R. Sahul, K. Snook, J. Luo, W. Hackenberger, and C. S. Lynch, "The strength of PIN-

- PMN-PT single crystals under bending with a longitudinal electric field," *Smart Mater. Struct.*, vol. 20, no. 5, art. no. 055006 2011.
- [16] T. Fett, S. Muller, D. Munz, and G. Thun, "Nonsymmetry in the deformation behaviour of PZT," *J. Mater. Sci. Lett.*, vol. 17, no. 4, pp. 261–265, 1998.
- [17] A. Nadai, *Theory of Flow and Fracture of Solids*. New York, NY: McGraw-Hill, 1950.
- [18] F. M. Discenzo, D. Chung, and K. A. Loparo, "Pump condition monitoring using self-powered wireless sensors," *Sound Vibrat.*, vol. 40, pp. 12–15, May 2006.
- [19] S.-H. Yoon, Y.-H. Lee, S.-W. Lee, and C. Lee, "Energy-harvesting characteristics of PZT-5A under gunfire shock," *Mater. Lett.*, vol. 62, no. 21–22, pp. 3632–3635, 2008.
- [20] S. Roundy and P. K. Wright, "A piezoelectric vibration based generator for wireless electronics," *Smart Mater. Struct.*, vol. 13, no. 5, pp. 1131–1142, 2004.
- [21] C. L. Zhang, "Harvesting magnetic energy using extensional vibration of laminated magnetolectric plates," *Appl. Phys. Lett.*, vol. 95, no. 1, art. no. 013511 2009.
- [22] H. Y. Lee, S. J. Zhang, and T. R. Shrout, "Development of high TC PMN-PZT piezoelectric single crystals by the solid-state crystal growth (SSCG) technique," in *17th IEEE Int. Symp. Applications of Ferroelectrics*, 2008, pp. 1–2.
- [23] S. Zhang, S.-M. Lee, D.-H. Kim, H.-Y. Lee, and T. R. Shrout, "Temperature dependence of the dielectric, piezoelectric, and elastic constants for $\text{Pb}(\text{Mg}_{1/3}\text{Nb}_{2/3})\text{O}_3$ - PbZrO_3 - PbTiO_3 piezocrystals," *J. Appl. Phys.*, vol. 102, no. 11, art. no. 114103, 2007.
- [24] A. Badel, A. Benayad, E. Lefevvre, L. Lebrun, C. Richard, and D. Guyomar, "Single crystals and nonlinear process for outstanding vibration-powered electrical generators," *IEEE Trans. Ultrason. Ferroelectr. Freq. Control*, vol. 53, no. 4, pp. 673–684, 2006.
- [25] K. Ren, Y. Liu, X. Geng, H. F. Hofmann, and Q. M. Zhang, "Single crystal PMN-PT/epoxy 1-3 composite for energy-harvesting application," *IEEE Trans. Ultrason. Ferroelectr. Freq. Control*, vol. 53, no. 3, pp. 631–638, 2006.
- [26] A. Erturk, O. Bilgen, and D. J. Inman, "Power generation and shunt damping performance of a single crystal lead magnesium niobate-lead zirconate titanate unimorph: Analysis and experiment," *Appl. Phys. Lett.*, vol. 93, no. 22, art. no. 224102, 2008.
- [27] S. E. Moon, S. Q. Lee, S.-K. Lee, Y.-G. Lee, Y. S. Yang, K.-H. Park, and J. Kim, "Sustainable vibration energy harvesting based on Zr-doped PMN-PT piezoelectric single crystal cantilevers," *ETRI J.*, vol. 31, no. 6, pp. 688–694, 2009.
- [28] H. A. Sodano, J. Lloyd, and D. J. Inman, "An experimental comparison between several active composite actuators for power generation," *Smart Mater. Struct.*, vol. 15, no. 5, pp. 1211–1216, 2006.
- [29] S. R. Anton, A. Erturk, N. Kong, D. S. Ha, and D. J. Inman, "An investigation on multifunctional piezoelectric composite spars for energy harvesting in unmanned aerial vehicles," presented at 17th Int. Conf. Composite Materials, Edinburg, UK, 2009.
- [30] S. R. Anton, A. Erturk, N. Kong, D. S. Ha, and D. J. Inman, "Self-charging structures using piezoceramics and thin-film batteries," in *ASME Conf. Smart Materials, Adaptive Structures and Intelligent Systems*, 2009, art. no. SMASIS2009-1368.
- [31] A. Erturk, S. R. Anton, and D. J. Inman, "Piezoelectric energy harvesting from multifunctional wing spars for UAVs—Part 1: Coupled modeling and preliminary analysis," *Proc. SPIE*, vol. 7288, art. no. 72880C–15, 2009.
- [32] *Standard Test Method for Flexural Strength of Advanced Ceramics at Ambient Temperature*, ASTM C 1161-02c, 2006.
- [33] *Standard Practice for Reporting Uniaxial Strength Data and Estimating Weibull Distribution Parameters for Advanced Ceramics*, ASTM C 1239-00, 2006.



Steven R. Anton received the B.S. degree in mechanical engineering from Michigan Technological University in 2006 and the M.S. and Ph.D. degrees in mechanical engineering from Virginia Tech in 2008 and 2011, respectively. He is currently a postdoctoral research associate at Los Alamos National Laboratory. His research interests include the use of smart materials for energy harvesting and structural health monitoring. He is a member of ASME and SPIE.



Alper Erturk is an Assistant Professor of mechanical engineering at the Georgia Institute of Technology. Since 2007, he has published more than 70 articles in refereed international journals and conference proceedings on smart materials and dynamic systems, and the book *Piezoelectric Energy Harvesting*. He is an elected member of the ASME Technical Committee on Adaptive Structures and Material Systems and the ASME Technical Committee on Vibration and Sound, and a member of ASME, AIAA, IEEE, SPIE, and SEM.

Dr. Erturk received his Ph.D. degree in engineering mechanics at Virginia Tech in 2009.



Daniel J. Inman received his Ph.D. degree from Michigan State University in mechanical engineering in 1980 and is Chair of the Department of Aerospace Engineering at the University of Michigan, as well as the C. L. "Kelly" Johnson Collegiate Professor. Since 1980, he has published eight books (on vibration, energy harvesting, control, statics, and dynamics), eight software manuals, 20 book chapters, more than 254 journal papers and 511 proceedings papers, has given 50 keynote or plenary lectures, has graduated 54 Ph.D. students,

and has supervised more than 75 M.S. degrees. He works in the area of applying smart structures to solve engineering problems, including energy harvesting, structural health monitoring, vibration suppression, and morphing. He is a Fellow of ASME, AIAA, IIAV, and AAM.